

This content has been downloaded from IOPscience. Please scroll down to see the full text.

Download details:

IP Address: 18.117.73.223

This content was downloaded on 26/04/2024 at 15:50

Please note that [terms and conditions apply](#).

You may also like:

[INVERSE PROBLEMS NEWSLETTER](#)

[Dual-Fluid Spray Process for Particle and Fluorocarbon-Polymer Removal in BEOL Applications](#)

Akihisa Iwasaki, Ayumi Higuchi, Kana Komori et al.

[Temperature-Dependent Interplay of Chemical Versus Electrochemical Electrolyte Oxidation at Ni-Rich Cathodes](#)

Leonhard Johannes Reinschluessel, Lennart Reuter and Hubert Andreas Gasteiger

Electroweak Baryogenesis (Second Edition)

An introduction

Graham White

---

## Chapter 5

### Gravitational waves from a strongly first-order electroweak phase transition

The discovery of gravitational waves by LIGO [1] ushered in a new way of looking at the Universe. Since the Universe is transparent to gravitational waves right back to the beginning of time, any event that generated gravitational waves back then can in principle be observed today. This is a remarkable advantage when we compare rival techniques to probe the early Universe. The Universe stops being transparent to light if we try and peer before a million years after its birth. Indirectly, we can peer back to when the Universe was a minute old by counting the abundances of light elements produced during big bang nucleosynthesis. However, even this early time corresponds to a temperature of a mere MeV. Current terrestrial colliders probe energies many orders of magnitude higher.

It has been long known that a strong first-order electroweak phase transition would leave a gravitational wave background. Given this is a necessary condition for electroweak baryogenesis, this is in principle exciting. It remains unclear though whether a signal that can be observed with projected technology is consistent with any model of electroweak baryogenesis. The issue is that projected technology requires a very strong transition generating a lot of latent heat. Such a large amount of latent heat released implies a huge amount of pressure accelerating the expansion of the bubble wall. If the bubble wall becomes ultra-relativistic, it might be difficult for charge asymmetries to diffuse as they need to in order to bias the sphalerons in front of the bubble wall. Whether this is possible in such a powerful transition as we would need to observe it is an open question of research (for a recent exploration see reference [2]). In this chapter, we will assume it is a possible discovery channel for the paradigm to justify its discussion.

Let us begin this chapter with a very brief, albeit slightly formal introduction to gravitational waves in general before diving into the specific example of phase transitions. Einstein's equation predicting the relationship between any source and gravity has the form

$$R_{\mu\nu} - \frac{1}{2}g_{\mu\nu}R = 8\pi T^{\mu\nu}. \quad (5.1)$$

The compact form of this equation is somewhat deceptive, we will need to manipulate this quite heavily in order to extract how a source corresponds to a gravitational wave spectrum. To begin with let us note that any gravitational wave sources we would realistically consider are small perturbations to a flat space-time metric

$$g_{\mu\nu} \sim \eta_{\mu\nu} + h_{\mu\nu}. \quad (5.2)$$

To first order in  $h$ , the linearized version of Einstein's equation has the form

$$\square \bar{h}_{\mu\nu} + \eta_{\mu\nu} \partial^\rho \partial^\sigma \bar{h}_{\rho\sigma} - \partial^\rho \partial_\nu \bar{h}_{\mu\rho} - \partial^\rho \partial_\mu \bar{h}_{\nu\rho} = -16\pi G T^{\mu\nu}. \quad (5.3)$$

Here we have used the usual shorthand that  $\bar{h}_{\mu\nu} = h_{\mu\nu} - \frac{1}{2}\eta_{\mu\nu}h$  and  $h = \eta^{\mu\nu}h_{\mu\nu}$ . At first glance, we have ten free parameters in a  $4 \times 4$  symmetric tensor, however the degrees of freedom are a lot less than 10. First, general relativity is invariant to diffeomorphisms of the form  $x^\mu \rightarrow x^\mu + \xi^\mu(x)$ . This can be used to greatly reduce the number of free parameters. In particular we can choose a gauge where

$$\partial^\nu \bar{h}_{\mu\nu} = 0. \quad (5.4)$$

This allows us to eliminate four free parameters, leaving us with six and the linearized Einstein equation becomes

$$\square \bar{h}_{\mu\nu} = -16\pi G T^{\mu\nu}. \quad (5.5)$$

For freely propagating gravitational waves away from their source, we can also ignore the stress energy tensor and we are free to make an additional coordinate transformation  $x^\mu \rightarrow x^\mu + \xi^\mu(x)$ , where  $\square \xi^\mu = 0$  without spoiling our gauge condition, to eliminate a further four free parameters. This leaves us with two free parameters left to match the number of degrees of freedom in a massless boson. We can use our freedom to make the trace vanish,  $h = 0$  and transverse in the sense that the wave vector is perpendicular to the metric,  $\partial^i h_{ij} = 0$ . The neat feature of the transverse traceless gauge is that you can project onto the transverse traceless gauge with a projection operator

$$\Lambda_{ij,kl} = P_{ik}P_{jl} - \frac{1}{2}P_{ij}P_{kl} \quad (5.6)$$

where

$$P_{ij} = \delta_{ij} - n_i n_j \quad (5.7)$$

and  $n$  is a unit vector pointing in the same direction as the wave vector of the gravitational wave. It is straight forward to verify that this operator is indeed a projector, as  $\Lambda_{ij,kl}\Lambda_{kl,mm} = \Lambda_{ij,mm}$  and it is transverse in its indices

$$n^i \Lambda_{ij,kl} = n^j \Lambda_{ij,kl} = \dots = 0. \quad (5.8)$$

Most importantly, the operator projects onto the transverse traceless gauge

$$h_{ij}^{TT} = \Lambda_{ij,kl} h_{kl}. \quad (5.9)$$

We can therefore use this projector to project out the part of the stress energy tensor that sources gravitational waves. Let us now proceed to derive the equation for the gravitational wave power spectrum. We will begin by writing everything as an expansion around the perturbation,  $h$ . For example, the Ricci tensor has the form<sup>1</sup>

$$R_{\mu\nu} = \bar{R}_{\mu\nu} + R_{\mu\nu}^1 + R_{\mu\nu}^2, \quad (5.10)$$

where the subscripts indicate the power in  $h$ . We can then separate the equation into low frequency and high frequency modes. The zeroth-order term depends upon the large distance behavior of the metric only, so it is a low frequency term. The term that is linear order depends on gravitons, so is a short distance or high frequency effect. The second-order term, however, can contain high frequency and low frequency modes. For example, two large wave number modes can combine to give a small wave number mode. The total low frequency part of the equation then has the form

$$\bar{R}_{\mu\nu} = -[R_{\mu\nu}^2]^{\text{Low}} + 8\pi G \left( T_{\mu\nu} - \frac{1}{2} g_{\mu\nu} T \right)^{\text{Low}}. \quad (5.11)$$

Using our gauge condition, we can write the Ricci scalar contribution to the above equation as

$$R_{\mu\nu}^2 = \frac{1}{2} \left( \frac{1}{2} \partial_\mu h_{\alpha\beta} \partial_\nu h^{\alpha\beta} + h^{\alpha\beta} \partial_\mu \partial_\nu h_{\alpha\beta} \right). \quad (5.12)$$

Taking the average and integrating by parts, we have

$$\langle R_{\mu\nu}^2 \rangle = -\frac{1}{4} \langle \partial_\mu h_{\alpha\beta} \partial_\nu h^{\alpha\beta} \rangle. \quad (5.13)$$

Thus, we can write the expectation value of the low frequency part of the Einstein equation as

$$\left\langle \left( T_{\mu\nu} - \frac{1}{2} g_{\mu\nu} T \right)^{\text{Low}} \right\rangle = \frac{1}{32\pi G} \langle \partial_\mu h_{\alpha\beta} \partial_\nu h^{\alpha\beta} \rangle. \quad (5.14)$$

To derive the power spectrum, we need to project the LHS onto the transverse traceless mode. We then need to take the 00 component which corresponds to the energy part of the spectrum. After taking the Fourier transform one has

$$\frac{dE}{d\Phi} = \frac{G}{2\pi^2} \Lambda_{ij,kl} \int d\omega \omega^2 \bar{T}_{ij}(\omega, \omega\hat{n}) \bar{T}_{kl}(-\omega, -\omega\hat{n}). \quad (5.15)$$

<sup>1</sup> For a more detailed discussion see reference [2].

Here  $\bar{T}_{ij}$  is the Fourier transform of the stress energy tensor and  $\Phi$  is the solid angle, usually denoted by the character  $\Omega$  which we will reserve for an abundance. Indeed, it is both convenient and customary to consider the abundance of gravitational waves in each frequency bin observed today,

$$\Omega = \frac{k}{\rho_c} \frac{d\rho_{GW}}{dk}, \quad (5.16)$$

where

$$\frac{d\rho_{GW}}{dkd\Phi} = 2G k^2 \Lambda_{ij,kl} \bar{T}_{ij} \bar{T}_{kl}. \quad (5.17)$$

The power spectrum above is written in terms of the wave number, which can easily be converted into a frequency when accounting for a factor of  $2\pi$  and a redshift factor. We will discuss this conversion later in the chapter. We now have the formalism needed to derive the gravitational wave spectrum so long as we can identify the relevant parts of the stress energy tensor. During a phase transition, there are three components to the stress energy tensor that leads to gravitational waves. Two of these are easy to model,

1. The contribution from the scalar shell which can be identified as the scalar field contribution to the stress energy tensor  $T_{\mu\nu}(x) = \partial_\mu\phi\partial_\nu\phi - g_{\mu\nu}\left[\frac{1}{2}\partial_\rho\phi\partial^\rho\phi - V\right]$ .
2. A contribution from soundwaves, where the plasma initially departs from its equilibrium state near the bubble wall then advances as sound shells that eventually collide. This contribution to the stress energy tensor has the form,  $T_{\mu\nu}(x) = \sum \int \frac{d^3k}{(2\pi)^3 2E} k_\mu k_\nu f(k) = (e + p)U_\mu U_\nu + g_{\mu\nu}p$  where  $w$  is the enthalpy,  $U$  the fluid velocity and  $p$  is the pressure.

The other contribution to gravitational waves is from turbulence—when the sound shells collide larger scales break down into smaller scales in a reasonably long lived process. This last contribution is very difficult to model (for an attempt, see reference [3]). Of the other two components, the sound shells dominate unless there is an extreme amount of energy in the bubble wall, a rare scenario that can be achieved with a great deal of supercooling (see for example reference [4]). It is also believed, though not proven until numerical simulations give better information, that the sound shell contribution dominates over turbulence as well. We therefore focus on this contribution.

We will need to derive the fluid velocity profile that arises from an expanding bubble. We will take the approximation that the gravitational wave spectrum arising from many sound shell collisions can be modelled as an incoherent superposition of the contribution of individual sound shells that are in free propagation after the phase boundaries collide [5, 6]. To derive the fluid velocity we use the equations that arises from the conserved current involving the stress energy tensor. That is, the stress energy tensor obeys the usual conservation law that its divergence vanishes  $T^{\mu\nu}_{;\mu} = 0$ . We can separate the two components by including a friction term that

captures the interaction between the fluid and the scalar shell. For simplicity we will work in Minkowski space, for this calculation performed in an expanding background see reference [7]. Since the expansion of the Universe is often quite slow compared to the time scale of the transition, ignoring the expansion of the Universe is often a reasonable approximation. The two components of the divergence of the stress energy tensor have the form,

$$T_{;\mu}^{\mu\nu}|_{\text{field}} = (\partial^2\phi)\partial^\nu\phi - \frac{\partial V}{\partial\phi}\partial^\nu\phi = \delta^\nu. \quad (5.18)$$

$$T_{;\mu}^{\mu\nu}|_{\text{fluid}} = \partial_\mu[(e+p)U^\mu U^\nu] + g^{\mu\nu}\partial_\mu p + \frac{\partial V}{\partial\phi} = -\delta^\nu. \quad (5.19)$$

It is trivial to see that the sums of the two terms are zero, as they should be, and the friction term can be modeled as the interaction between the fluid and the field gradients  $\delta^\nu = \eta U^\mu \partial_\mu \phi \partial^\nu \phi$ . Let us define a couple of shorthands for notational compactness

$$Z^i = \gamma^2(e+p)v^i, \quad E = e\gamma. \quad (5.20)$$

We will also take the fluid velocity to have the form,  $U^\mu = \gamma(v, \hat{v}^i)$ . We can write the equations of motion arising from the divergence of the stress energy tensor in spatial and temporal components as

$$-\ddot{\phi} + \nabla^2\phi - \frac{\partial V}{\partial\phi} = \eta\gamma(\dot{\phi} + \bar{v} \cdot \nabla\phi), \quad (5.21)$$

$$\dot{Z}^i + \nabla \cdot (\bar{v}\nabla Z^i) + \partial_i p + \frac{\partial V}{\partial\phi}\partial_i\phi = -\eta\gamma(\dot{\phi} + \bar{v} \cdot \nabla\phi)\partial_i\phi, \quad (5.22)$$

$$\dot{E} + p(\dot{\gamma} + \nabla \cdot \gamma\bar{v}) + \nabla \cdot (E\bar{v}) - \gamma\frac{\partial V}{\partial\phi}(\dot{\phi} + \bar{v} \cdot \nabla\phi) = \eta\gamma^2(\dot{\phi} + \bar{v} \cdot \nabla\phi)^2, \quad (5.23)$$

$$\begin{aligned} & \gamma^2(\dot{v} + \hat{v} \cdot v^2)(e+p) + v\dot{p} + \hat{v} \cdot \nabla p + \frac{\partial V}{\partial\phi}(v\dot{\phi} + \hat{v} \cdot \nabla\phi) \\ & = -\eta\gamma(v\dot{\phi} + \hat{v} \cdot \phi)(\dot{\phi} + v \cdot \nabla\phi). \end{aligned} \quad (5.24)$$

Unless the bubble walls runaway such that the boost factor is very large, the field components of the above equation can be safely ignored and we have the significantly simpler system of equations

$$\dot{Z}^i + \nabla \cdot (\bar{v}\nabla Z^i) + \partial_i p = 0, \quad (5.25)$$

$$\dot{E} + p(\dot{\gamma} + \nabla \cdot \gamma\bar{v}) + \nabla \cdot (E\bar{v}) = 0, \quad (5.26)$$

$$\gamma^2(\dot{v} + \hat{v} \cdot v^2)(e+p) + v\dot{p} + \hat{v} \cdot \nabla p = 0. \quad (5.27)$$

We can make two further simplifications. First let us assume spherically symmetric sound shells, then we can note that because there is no characteristic scale in the problem, the solution should only depend on the ratio  $\xi = r/t$ . We can then denote  $v(\xi)$  as the fluid velocity in the rest frame of the center of the bubble and the gradients become

$$U_\mu \partial^\mu = \frac{\gamma}{t} (\xi - v) \partial_\xi. \quad (5.28)$$

We can then combine our equations into a single equation which has the form

$$2 \frac{v}{\xi} = \gamma^2 (1 - v\xi) \left( \frac{(\xi - v)^2}{c_s^2 (1 - \xi v)^2} - 1 \right) \partial_\xi v. \quad (5.29)$$

Here,  $c_s^2$  is the speed of sound, given by  $c_s^2 = dp/de$ , which we take to be its equilibrium value of  $1/3$  throughout. For a more precise treatment see reference [7]. To solve this equation, we require boundary condition at the bubble wall. We can use the bag equation of state where the pressure and energy are made continuous at the boundary by means of a bag constant

$$p_+ = \frac{1}{3} a_+ T_+^4 - \epsilon, \quad p_- = \frac{1}{3} a_- T_-^4, \quad (5.30)$$

$$e_+ = a_+ T_+^4 + \epsilon, \quad e_- = a_- T_-^4. \quad (5.31)$$

where  $\epsilon$  and  $\frac{1}{3} a_x T_x^4$  gives the Stephann Boltzmann pressure in each phase, that is

$$a = \frac{\pi^2}{30} \sum n_b + \frac{7}{8} n_f, \quad (5.32)$$

and  $n_{b/f}$  are the number of relativistic bosonic/fermionic degrees of freedom in each phase, respectively. We can then match the stress energy tensor at the bubble wall boundary

$$w_+ v_+^2 \gamma_+^2 + p_+ = w_- v_-^2 \gamma_-^2 + p_- \quad (T_+^{rr} = T_-^{rr}), \quad (5.33)$$

$$w_+ v_+ \gamma_+^2 = w_- v_- \gamma_-^2 \quad (T_+^{rt} = T_-^{rt}). \quad (5.34)$$

In the above we put the matching condition we were using in the parenthesis. From these two equations we can derive

$$v_+ v_- = \frac{p_+ - p_-}{e_+ - e_-}, \quad \frac{v_+}{v_-} = \frac{p_+ + e_-}{e_+ + p_-}. \quad (5.35)$$

Using these boundary conditions, one can acquire a solution for the velocity field. It is not difficult to solve these equations numerically, however, we will later use a fit for the fluid velocity. Let us conclude by sketching the derivation of the gravitational wave power spectrum. We will parameterize the power spectrum as follows

$$\frac{d\rho_{GW}}{d\text{Log}k} = \frac{1}{32\pi G} \frac{k^3}{2\pi^2} P_h(k, t). \quad (5.36)$$

Assuming the fluid shear stress, which we denote by  $\tau^{ij} = (e + p)v^i v^j$ , dominates the spatial components we can make an assumption of homogeneity and write the transverse traceless component of the two point unequal time correlator by parametrizing it as

$$\Lambda_{ij,kl} \langle \tau_{k_1}^{ij}(t_1) \tau_{k_2}^{kl}(t_2) \rangle = \Pi^2(k_1, t_1, t_2) (2\pi)^3 \delta(k_1 + k_2). \quad (5.37)$$

Here the delta function ensures homogeneity which can be seen as follows: take the Fourier transform of both momenta variables and after the application of the delta function, it will only be a function of the relative coordinate. We will average over a period  $T$  for time scales much longer than the characteristic period of the gravitational waves,

$$P_{\tilde{h}}(k, t) = (16\pi G)^2 \int_0^T dt_1 dt_2 \frac{\cos[k(t_1 - t_2)]}{2} \Pi^2(k, t_1, t_2). \quad (5.38)$$

Let us assume the unequal time correlator is only a function of the difference in times. We can further assume the fluid stress is characterized by a typical length scale,  $L_f$ , and does not evolve after creation. Under these assumptions we can parametrize

$$\Pi^2(k_2, t_1, t_2) = ((\bar{p} + \bar{e}) \bar{U}_f^2)^2 L_f^3 \tilde{\Pi}^2(kL_f, k(t_1 - t_2)), \quad (5.39)$$

where  $\tilde{\Pi}$  is a dimensionless function and the bars indicate averages, then

$$P_{GW}(kL_f) = \frac{1}{k} \frac{1}{L_f} \int dz \frac{\cos[z]}{2} \tilde{\Pi}^2(kL_f, z). \quad (5.40)$$

In the above  $k(t_1 - t_2) = z$ . Averaging over the lifetime,  $\tau_v$ , and identifying the average energy density as the critical energy density  $\bar{e} = \rho_c = 4H^2/8\pi G$ , we can write the gravitational wave abundance as [5, 6, 8]

$$\Omega_{GW} = 3 \left( 1 + \frac{\bar{p}}{\bar{e}} \right)^2 \bar{U}_f^4 (H\tau_v) (HL_f) \frac{(kL_f)^3}{2\pi^2} P_{GW}(kL_f). \quad (5.41)$$

The factor  $(H\tau_v)$  is often less than one and is a suppression factor from the finite lifetime of the sound wave. A careful derivation on an expanding background gives a slightly different factor (see reference [7]) which we will simply quote at the end. The function  $P_{GW}(kL_f)$  needs to be numerically solved, as does the average fluid velocity. There are, however, some good fits for both of these in terms of thermal parameters in the phase transition. We will return to this shortly. First let us describe the spectrum in terms of thermal parameters. The first component to consider is the redshift factor. The total energy dilutes as radiation, whereas the critical energy density will only dilute as radiation until matter domination, after which it dilutes slower. This means the relationship between the gravitational wave abundance at the time compared to today is given by

$$h^2 \Omega_{GW}(z = z_0, f) \leftrightarrow h^2 \left( \frac{z_*}{z_0} \right)^4 \left( \frac{H_*}{H_0} \right)^2 \Omega_{GW}(z = z_*, z_0 f / z_*). \quad (5.42)$$



Here and throughout, the starred subscript refers to the time of percolation which occurs approximately when the effective action of the bounce profile discussed in chapter 4, is two orders of magnitude larger than the temperature (a more exact approach is to calculate the volume fraction in each phase and take the temperature when there is an order one fraction in the low temperature phase). After applying this redshift factor and numerically solving for the power spectrum one finds the fit

$$h^2\Omega_{GW}(f) = 4.98 \times 10^{-5} \left( \frac{100}{g_*(T_*)} \right)^{1/3} \Gamma^2 \bar{U}_f^A(H_* R_*) A S(f) \Upsilon(t_{SW}). \quad (5.43)$$

Here the numerical factor  $A = 0.058$ ,  $\Gamma^2 = 4/3$ , the spectral form is

$$S(f) = \left( \frac{f}{f_{SW}} \right)^3 \left[ \frac{7}{4 + 3(f/f_{SW})^2} \right]^{7/2}, \quad (5.44)$$

which peaks at the frequency

$$f_{SW} = 2.65 \times 10^{-5} \text{Hz} \frac{1}{v_w} \left( \frac{g_*(T_*)}{100} \right)^{1/6} \left( \frac{T_*}{100 \text{ GeV}} \right)^{z_p} \frac{1}{10 H_* R_*}, \quad (5.45)$$

$z_p \sim 7$  is a simulation factor and the suppression factor from the finite time of the soundwaves takes the form

$$\Upsilon(t_{SW}) = 1 - \frac{1}{\sqrt{1 + 2\tau_{SW}H_*}}, \quad (5.46)$$

and of course  $H_*$  is the value of Hubble at the time of the phase transition. We now have several thermal parameters left to calculate. The bubble wall velocity is by far the most complicated and we will tackle it in chapter 8. To properly calculate the mean bubble separation,  $R_*$ , one should calculate the cubed route of the bubble number density at the time of percolation. From this one can estimate the lifetime of the soundwaves  $\tau_{SW} = R_*/\bar{U}_f$ . A more approximate approach that agrees to within around 20% of the true value is to take the derivative of the effective action of the bounce profile

$$R_* = (8\pi)^{1/3} \frac{v_w}{\beta}, \quad \frac{\beta}{H_*} = T \left. \frac{d(S_E/T)}{dT} \right|_{T_*}. \quad (5.47)$$

The fluid velocity also can be approximated in terms of the trace anomaly,

$$\bar{U}_f^2 = \frac{3}{4} \kappa \alpha, \quad (5.48)$$

where the trace anomaly is

$$\alpha = \frac{\Delta V - T d\Delta V/dT}{\rho_c}, \quad (5.49)$$

and  $\Delta V$  is the difference in the effective potential between the two phases, defined as to be positive semi-definite. Finally, the efficiency factor has the form [9]

$$\kappa = \begin{cases} \frac{\alpha}{0.73 + 0.083\sqrt{\alpha} + \alpha}, & v_w \sim 1 \\ \frac{v_w^{6/5} 6.9\alpha}{1.36 - 0.037\sqrt{\alpha} + \alpha}, & v_w < 0.1 \\ \frac{\alpha^{2/5}}{0.017 + (0.997 + \alpha)^{2/5}}, & v_w = c_s \end{cases} \quad (5.50)$$

Of course, it is more accurate to numerically solve the fluid equations. Beyond this, numerical simulations seem to indicate that the sound shell model does a poor job capturing the suppression from energy that goes into vorticity modes. Unfortunately, this effect can only be captured numerically using a fit [10]. Beyond this, the power spectrum has two observables in its peak frequency and amplitude as the sound shell model predicts a spectral form that is independent of the thermal parameters. This mapping of two observables from four thermal parameters which are in turn derived from any number of multiparameter models can make the inverse problem look at first formidable. Simulations, however, seem to indicate a more promising picture, where the precise shape of the power spectrum is sensitive to all four thermal parameters, indicating that any observation of a gravitational wave signature would contain a lot of information about the underlying model that produced it [11]. Of course, this piece of good news is also bad news for phenomenologists who might wish for a simple mapping between their model and the predicted gravitational wave signal, simulations are formidably expensive! Still, this is a work in progress and the above spectral form should be taken with a grain of salt as a starting point in understanding the signals from a given theory (figure 5.1). An example of how the sound shell model can give a

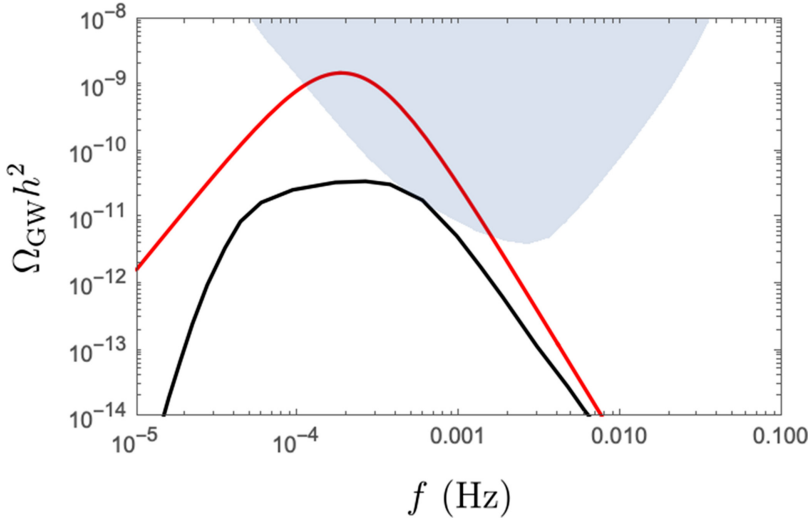


**Figure 5.1.** The gravitational wave spectrum for a benchmark as predicted from simulations (black) versus the spectrum predicted by the sound shell model (red) compared to the sensitivity of LISA (blue) [12]. The shape and amplitude differ dramatically for this benchmark which demonstrates the need for further development in predicting the gravitational wave spectrum. Benchmark and simulation data taken from reference [11].

different prediction of the spectrum compared to a simulation is given below. Note the existence of the breakpoint and the peak allows one to in principle reconstruct four thermal parameters.

## References

- [1] Abbott B PLigo Scientific and Virgo Collaborations *et al* 2016 Observation of gravitational waves from a binary black hole merger *Phys. Rev. Lett.* **116** 061102
- [2] Maggiore M 2008 *Gravitational Waves* (Oxford: Oxford University Press)
- [3] Caprini C, Durrer R and Servant G 2009 The stochastic gravitational wave background from turbulence and magnetic fields generated by a first order phase transition *JCAP* **12** 024
- [4] Ellis J, Lewicki M, No J and Vaskonen V 2019 Gravitational wave energy budget in strongly supercooled phase transitions *JCAP* **06** 024
- [5] HindMarsh M 2014 Gravitational waves from the sound of a first order phase transition *Phys. Rev. Lett.* **112** 041301
- [6] HindMarsh M, Huber S and Rummukainen K 2015 Numerical simulations of acoustically generated gravitational waves at a first order phase transition *Phys. Rev. D* **92** 12
- [7] Guo H, Sinha K, Vagie D and White G 2021 Phase transitions in an expanding Universe: stochastic gravitational waves in standard and non-standard histories *JCAP* **01** 001
- [8] Ellis J, Lewicki M and No J 2019 On the maximal strength of a first order electroweak phase transition and its gravitational wave signal *JCAP* **04** 003
- [9] Espinosa J, Konstandin T and Geraldine S 2010 Energy budget of cosmological first order phase transitions *JCAP* **06** 028
- [10] Cutting D, HindMarsh M and Weir D 2019 Vorticity, kinetic energy, and suppressed gravitational wave production in strong first order phase transitions *Phys. Rev. Lett.* **125** 021302
- [11] Gowling C and HindMarsh M 2021 Observational prospects for phase transitions at LISA: Fisher matrix analysis *JCAP* **10** 039
- [12] Caprini C *et al* 2020 Detecting gravitational waves from cosmological phase transitions with LISA: an update *JCAP* **03** 024